ISSN 1990-3413, Astrophysical Bulletin, 2018, Vol. 73, No. 2, pp. 241–248. © Pleiades Publishing, Ltd., 2018.
Original Russian Text © V.L. Afanasiev, A.V. Ipatov, 2018, published in Astrofizicheskii Byulleten', 2018, Vol. 73, No. 2, pp. 250–258.

Observations of Near-Earth Asteroids in Polarized Light

V. L. Afanasiev[1*] and A. V. Ipatov[2]

[1]*Special Astrophysical Observatory, Russian Academy of Sciences, Nizhnii Arkhyz, 369167 Russia*
[2]*Institute of Applied Astronomy of the Russian Academy of Sciences, St. Petersburg, 191187 Russia*

Received December 1, 2017; in final form, March 22, 2018

Abstract—We report the results of position, photometric, and polarimetric observations of two near-Earth asteroids made with the 6-m telescope of the Special Astrophysical Observatory of the Russian Academy of Sciences. 1.2-hour measurements of the photometric variations of the asteroid 2009 DL46 made on March 8, 2016 (approximately $20^{\rm m}$ at a distance of about 0.23 AU from the Earth) showed a $0\overset{\rm m}{.}2$-amplitude flash with a duration of about 20 minutes. During this time the polarization degree increased from the average level of 2–3% to 14%. The angle of the polarization plane and the phase angle were equal to $113° \pm 1°$ and 43°, respectively. Our result indicates that the surface of the rotating asteroid (the rotation period of about 2.5 hours) must be non-uniformly rough. Observations of another asteroid—1994 UG—whose brightness was of about $17^{\rm m}$ and which was located at a geocentric distance of 0.077 AU, were carried out during the night of March 6/7, 2016 in two modes: photometric and spectropolarimetric. According to the results of photometric observations in Johnson's B-, V-, and R-band filters, over one hour the brightness of the asteroid remained unchanged within the measurement errors (about $0\overset{\rm m}{.}02$). Spectropolarimetric observations in the 420–800 nm wavelength interval showed the polarization degree to decrease from 8% in the blue part of the spectrum to 2% in the red part with the phase angle equal to 44°, which is typical for S-type near-Earth asteroids.

DOI: 10.1134/S1990341318020104

Key words: *minor planets, asteroids: individual: DL46—minor planets, asteroids: individual: 1994 UG—techniques: polarimetric*

1. INTRODUCTION

Investigation of the dynamical and physical properties of near-Earth asteroids provides not only to study their nature, but also assess the danger of their eventual collision with the Earth. Radar observations can provide images and study translational and rotational motions of these celestial bodies with an accuracy unachievable with optical methods, which, on the other hand, can be used to study the physical and mineralogical properties of these bodies.

The primary task of optical observations of asteroids is to measure their albedos, which are determined both by the roughness of the surface and the composition of the asteroid matter. Traditional photometric and spectroscopic methods are oriented toward searching for differences between the spectrum of the asteroid and the solar spectrum, which are quite small (1–2%) [1]. Polarimetric techniques, which allow physical properties of asteroids to be determined from observations at optical wavelengths, are more promising. Polarimetric observations of asteroids provide information about the geometric albedos of asteroids and can serve as a source of indirect data about the typical sizes of particles of the surface regolith. The importance of polarimetry as a powerful tool (along with spectrophotometry) was pointed out in [2–5]. A single polarimetric observation of an asteroid is not sufficient for determining the properties of the body because polarization pattern depends on phase angle. Only single observations have been made for most of the asteroids and the data about the polarization of asteroids over a wide range of phase angles is available only for a small fraction of such objects [6].

For obvious reasons, near-Earth asteroids (NEA) are of particular interest. These asteroids can be observed at large phase angles, where polarization is determined by scattering on individual particles and by the surface albedo. So far, polarimetric observations at phase angles greater than 90° have been made only for three NEAs: (1685) Toro [7], and (4179) Toutatis [8], and (23187) 2000 PN_9 [9]. These are so-called S-type asteroids and they have rather similar polarization properties: $P_{\max} = 7.7$–8.5% and

*E-mail: vafan@sao.ru

$\alpha_{\max} = 103°–110°$. Maximum polarization was also observed in E-type asteroid 33342 (1998 WT24) [10]. Despite their limited amount, the currently available data about NEAs show that even single polarimetric measurements can be used to distinguish asteroids with low, moderate, and high albedos. The study of photometric variations and their comparison with radio data appears to be of great importance. The ultimate aim of the study of NEAs includes both the determination of their dynamical parameters and surface properties.

In this paper we report the results of polarimetric and photometric observations of two faint near-Earth asteroids made with the 6-m telescope of the Special Astrophysical Observatory of the Russian Academy of Sciences.

2. OBSERVATIONS

Observations were made with SCORPIO-2 universal spectrograph [11] mounted in the prime focus of the 6-m telescope of the Special Astrophysical Observatory of the Russian Academy of Sciences. The following operation modes of the spectrograph were employed:

- direct imaging in the BVR filters of Johnson's system;
- V-band polarimetry using dichroic polaroid;
- low-resolution ($R \sim 500$) spectropolarimetry in the 0.4–0.9 μm wavelength interval.

The detector employed was a 4096×2048 EEV 42-90 CCD. The image scale in the detector plane was $0''.357$ px with a pixel size of 27 μm (binning=2).

In early 2016, when test observations were planned on the 6-m telescope, two asteroids—DL46 and 1994 UG could be observed. Observations were made in March during director's discretionary nights. Below we report the results of observations of both asteroids.

2.1. Observations of Asteroid DL46

According to is ephemeris, asteroid DL46 was rather faint (about 20^{m}) and located at a distance of 0.23 AU from the Earth. Visibility conditions (the Moon) made it possible to observe the asteroid only in the evening of March 8, 2016. Because of the faintness of the object only V-band polarimetry with a rotating polarimeter was performed using the method developed by V. G. Fesenkov. Table 1 presents the log of observations, which gives: the name of the FITS file of the image, the Universal time of the mid-exposure, angle of polaroid angle, seeing in arcsec, zenith angle, measured equatorial coordinates of the asteroid

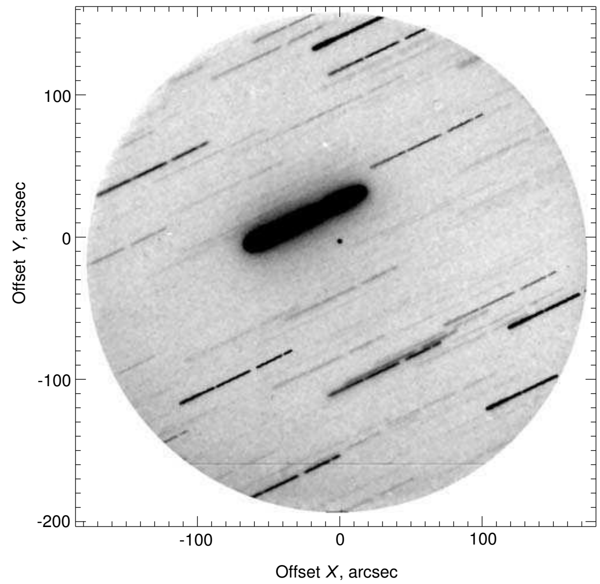

Fig. 1. Stacked V-band image of the asteroid (with a total exposure of 3600 s).

at mid-exposure time and their measurement errors. Exposures were the same for all images and equal to 100 s. Guiding was made via Metcoff method using lunar-planetary drive of the automatic control system of the 6-m telescope of the Special Astrophysical Observatory of the Russian Academy of Sciences. Figure 1 shows the stacked image, which illustrates the quality of the guiding of the asteroid. For photometric calibration we took a series of images of the open cluster NGC 2420. We used standard `DAOPHOT` procedures to reduce the data.

2.1.1. Position Measurements

We performed astrometric reduction of each image using USNO-2.0 catalog in the format of the Guide Star Catalog [12] and wrote standard nonlinear astrometric structure inti each FITS-file header. The average astrometric accuracy of the reduction of a single frame is of about $0''.3$. The results of position measurements of the asteroid DL46 are given in columns (7) and (8) of Table 1 and columns (9) and (10) give the errors of astrometric reduction.

2.1.2. Polarimetry

We already described the technique of the reduction of polarimetric data obtained in observations with a polaroid in our earlier paper [13]. The most critical factor in polarization measurements made using Fesenkov's method is atmospheric stability. Figure. 2a shows the brightness variations of the reference star with zero polarization in the field of DL46 for three polaroid angles and the corresponding variations of

Table 1. Polartimetric observations of the asteroid DL46 on March 8, 2016

File	UT hh mm ss.ss	Angle, deg	Seeing, arcsec	z, deg	RA(2000), hh mm ss.ss	Dec(2000), dd mm ss.ss	Err RA, arcsec	Err Dec, arcsec
(1)	(2)	(3)	(4)	(5)	(6)	(7)	(8)	(9)
s13880203	16 36 21.75	−60	1.0	39	10 30 39.953	+56 40 34.19	0.21	0.10
s13880204	16 38 18.06	0	1.0	39	10 30 39.780	+56 40 36.41	0.18	0.37
s13880205	16 40 13.37	+60	0.8	38	10 30 39.699	+56 40 38.11	0.13	0.23
s13880206	16 43 12.94	−60	0.8	38	10 30 39.453	+56 40 41.84	0.16	0.36
s13880207	16 45 09.25	0	0.8	38	10 30 39.341	+56 40 42.95	0.14	0.27
s13880208	16 47 03.56	+60	0.8	38	10 30 39.220	+56 40 45.56	0.17	0.46
s13880209	16 49 06.88	−60	0.8	37	10 30 39.084	+56 40 47.80	0.19	0.28
s13880210	16 51 03.29	0	0.8	37	10 30 38.960	+56 40 49.42	0.22	0.26
s13880211	16 52 59.59	+60	0.8	37	10 30 38.796	+56 40 51.05	0.16	0.15
s13880212	16 55 01.00	−60	0.8	36	10 30 38.737	+56 40 53.01	0.29	0.24
s13880213	16 56 55.30	0	0.8	36	10 30 38.584	+56 40 55.11	0.25	0.26
s13880214	16 58 51.40	+60	0.8	36	10 30 38.522	+56 40 56.90	0.22	0.18
s13880215	17 04 50.92	−60	0.8	35	10 30 38.103	+56 41 03.58	0.22	0.21
s13880216	17 06 47.13	0	0.8	35	10 30 38.033	+56 41 04.81	0.28	0.35
s13880217	17 08 41.43	+60	0.8	35	10 30 37.845	+56 41 07.17	0.18	0.39
s13880218	17 10 44.84	−60	0.8	34	10 30 37.683	+56 41 08.60	0.24	0.21
s13880219	17 12 40.14	0	0.8	34	10 30 37.546	+56 41 11.30	0.26	0.40
s13880220	17 14 36.54	+60	0.8	34	10 30 37.445	+56 41 12.94	0.22	0.32
s13880221	17 16 39.96	−60	0.8	33	10 30 37.384	+56 41 15.07	0.16	0.24
s13880222	17 18 34.26	0	0.8	33	10 30 37.191	+56 41 17.53	0.29	0.38
s13880223	17 20 29.57	+60	0.8	33	10 30 37.129	+56 41 18.74	0.27	0.23
s13880224	17 22 31.88	−60	0.8	33	10 30 36.961	+56 41 21.27	0.18	0.19
s13880225	17 24 29.18	0	0.8	32	10 30 36.829	+56 41 23.21	0.25	0.22
s13880226	17 26 23.59	+60	0.8	32	10 30 36.699	+56 41 25.28	0.27	0.21
s13880227	17 29 34.16	−60	0.8	32	10 30 36.456	+56 41 28.87	0.24	0.24
s13880228	17 31 28.36	0	0.8	31	10 30 36.372	+56 41 30.33	0.20	0.26
s13880229	17 33 22.56	+60	0.8	31	10 30 36.264	+56 41 32.67	0.20	0.24
s13880230	17 35 24.77	−60	0.8	31	10 30 36.126	+56 41 34.30	0.22	0.29
s13880231	17 37 43.09	0	0.8	31	10 30 35.979	+56 41 36.82	0.25	0.27
s13880232	17 39 38.50	+60	0.8	30	10 30 35.823	+56 41 38.39	0.20	0.27
s13880233	17 41 39.91	−60	0.8	30	10 30 35.684	+56 41 41.15	0.25	0.29
s13880234	17 43 36.22	0	1.1	30	10 30 35.568	+56 41 42.65	0.28	0.29
s13880235	17 45 31.53	+60	1.1	29	10 30 35.495	+56 41 45.06	0.21	0.18
s13880236	17 47 32.85	−60	1.1	29	10 30 35.305	+56 41 46.59	0.23	0.29
s13880237	17 49 29.16	0	1.1	29	10 30 35.144	+56 41 49.03	0.29	0.19
s13880238	17 51 24.37	+60	1.1	29	10 30 35.052	+56 41 50.87	0.21	0.23

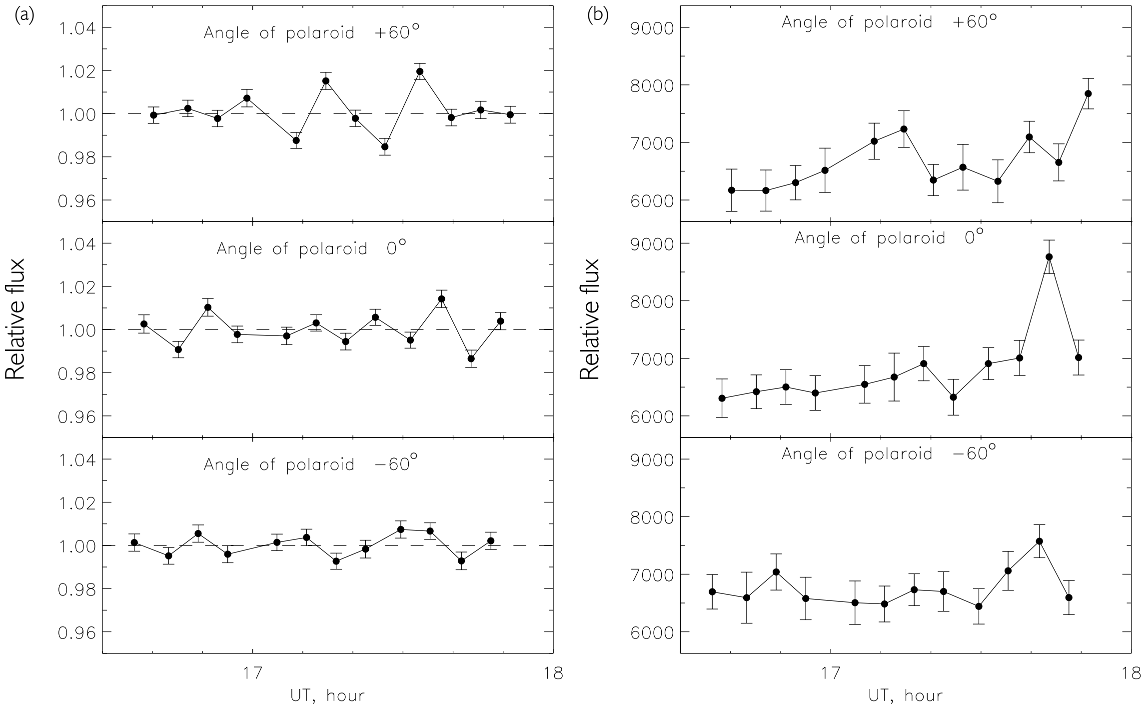

Fig. 2. Variations of the flux of the reference star (a) and asteroid DL46 (b) in different polarization channels.

the flux of the object studied (Fig. 2b). It can be concluded that the variations of the flux of DL46 in different polarization channels during the observing time (one hour) reach 40–50%, which exceeds appreciably both atmospheric variations (1.5%) and random measurement errors (4%), which are determined by the statistics of photometric counts.

Given the measured intensities at three polaroid angles—$I(x, y)_0$, $I(x, y)_{-60}$, and $I(x, y)_{+60}$, we can compute Stokes parameters Q and U at any image point with the coordinates (x, y) up to a rotation. We use the following formulas:

$$Q(x, y) = \frac{2I(x, y)_0 - I(x, y)_{-60} - I(x, y)_{+60}}{I(x, y)_0 + I(x, y)_{-60} + I(x, y)_{+60}}$$

$$U(x, y) = \frac{1}{\sqrt{3}} \frac{I(x, y)_{+60} - I(x, y)_{-60}}{I(x, y)_0 + I(x, y)_{-60} + I(x, y)_{+60}}. \quad (1)$$

We then use the well-known formula

$$P = \sqrt{Q^2 + U^2}, \quad PA = PA_{\text{slit}} - \frac{1}{2}\arctan\frac{U}{Q} + PA_0 \quad (2)$$

to compute the degree of linear polarization, P, and the position angle of the polarization plane, PA. Here PA_{slit} and PA_0 are instrumental constants. Figure 3 shows the observed variation with time of the following parameters of the linear polarization of asteroid DL46: integrated magnitude (Stokes parameter I); normalized Stokes parameters Q and U; linear polarization degree P, and position angle of the polarization plane, PA. As is evident from the figure, the flux from the asteroid varied only slightly and appreciable brightening can be observed only during 20 minutes at the last three data points of our series when the flux increased by 0.2^{m}, which exceeds variations of atmospheric transparency by almost a factor of ten (see Fig. 2). However, it is more surprising that that during this time the degree of linear polarization increased from the average level of 2–3%. The angle of the polarization plane during this time remained unchanged and coincided with the phase angle of asteroid according to ephemeris (about 42°) within the errors. The sharp increase of polarization must be due to the inhomogeneity of the asteroid surface, e.g., to the presence of smooth surface areas like basalt plates.

2.2. Observations of Asteroid 1994 UG

According to the ephemeris of asteroid 1994 UG, during the observing night of March 6, 2016 it was quite bright (about 17^{m}) and it was located at a distance of 0.077 AU from the Earth. We not only

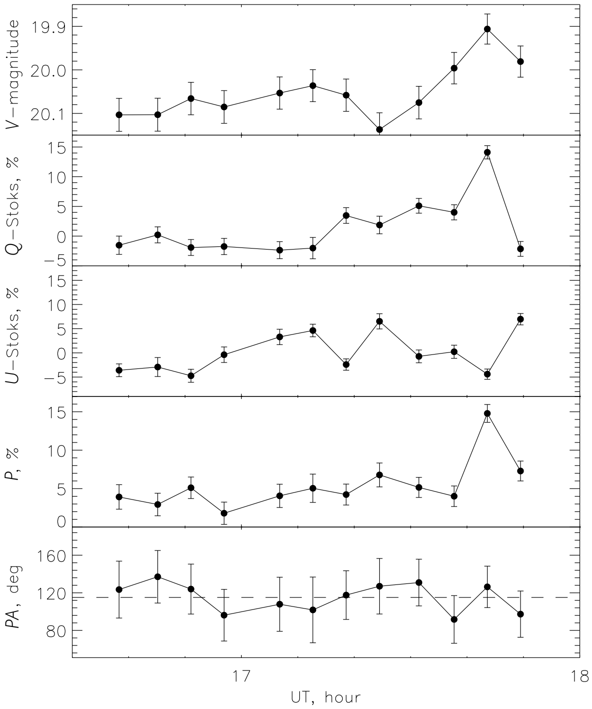

Fig. 3. Variation of the polarization parameters of asteroid DL46.

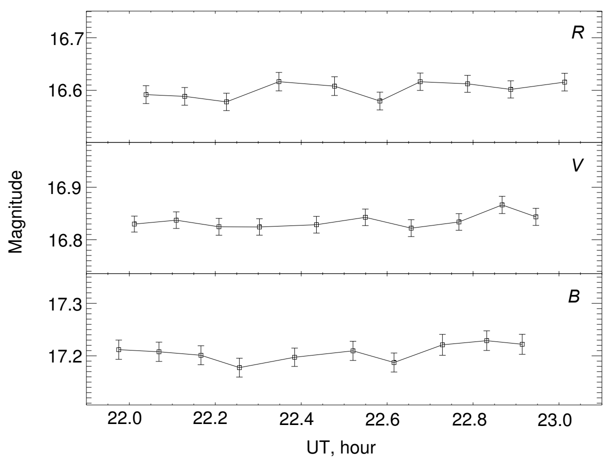

Fig. 4. Photometric variations of asteroid 1994 UG in different filters.

measured its brightness and position in different filters, but also studied its spectrum in polarized light. Table 2 presents the results of our position and photometric observations' of asteroid 1994 UG including: the number of the file; Universal time of mid-exposure; exposure; filter; zenith angle; seeing; measured coordinates of the object; error of astrometric reduction, and magnitude.

2.2.1. Astrometry and Photometry

Astrometric reduction was performed in the same way as in the case of asteroid DL46.

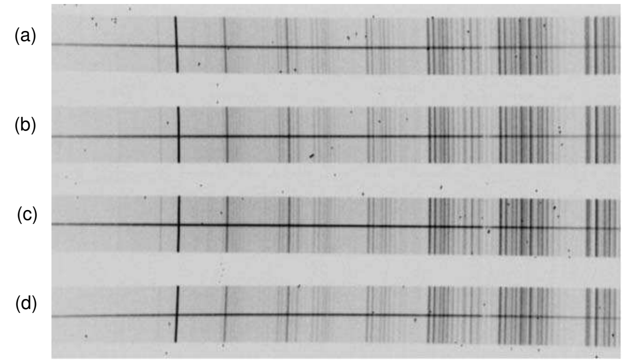

Fig. 5. Spectra asteroid 1994 UG without sky background subtraction obtained with double Wollastone analyzer with a 180-s exposure on on March 6, 2016 (UT 23:39). The angles of the polarization plane selected in the spectra are equal to 0° (a), 90° (b), 45° (c), and 135° (d).

Photometric measurements were conducted in three color bands of the Johnson system: B, V, and R ($\lambda_{\rm eff} \sim 435$ nm, 555 nm, and 700 nm, respectively). Atmospheric transparency was sufficiently good. Exposure for each filter was chosen so as to provide equal accuracy in all filters. One of the problems in photometric observations was that in more than half of all acquired frames the asteroid images were superimposed by images of faint stars, which made it difficult to measure sky background for further subtraction and introduced systematic errors into photometric estimates. In some of the cases errors could be as large as $0.2–0.3^{\rm m}$. For correct deblending if images we used methods of aperture photometry, which reduced systematic errors down to several hundredths of a magnitude. We list the results of photometric measurements for each observing time in Table 2. Figure 4 shows the variations of the asteroid brightness with time.

As is evident from the figure, we found no significant variations of the flux and color index exceeding the variations of atmospheric transparency (3% or $0.03^{\rm m}$).

2.2.2. Spectropolarimetry

We performed spectropolarimetric observations of asteroid 1994 UG on the 6-m telescope of the Special Astrophysical Observatory of the Russian Academy of Sciences using SCORPIO-2 spectrograph with a double Wollastone analyzer, which allows simultaneously obtaining four spectra in different planes of the oscillation of the electric vector of the visible electromagnetic radiation—0°, 90°, 45°, and 135°. The height of the spectrograph slit was 1′, making it possible to reliably subtract the night-sky background. We took a total of five spectra with 180-s exposures using a 940 lines mm^{-1} phased holographic grating operating in the 420–850 nm wavelength

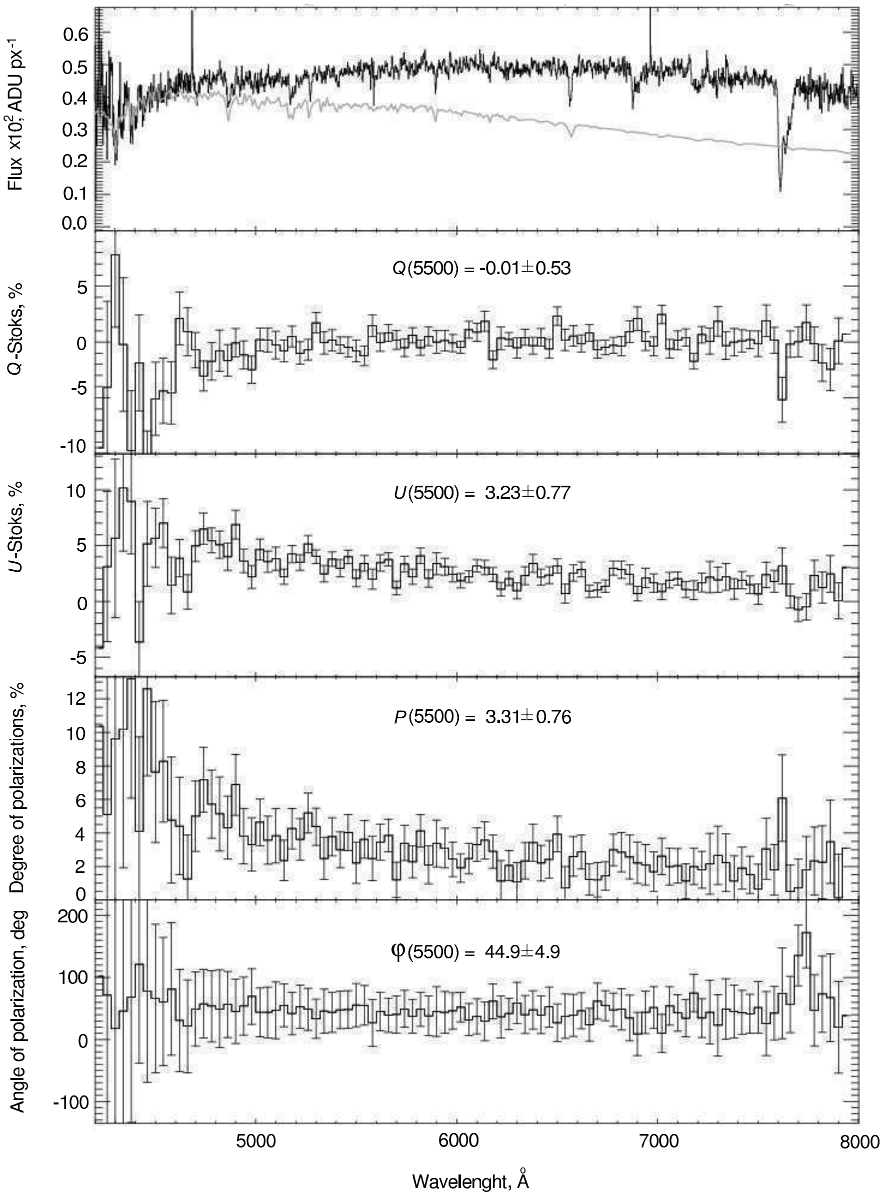

Fig. 6. Polarization parameters in the spectrum of asteroid 1994 UG .

range. The slit width and seeing were equal to $2''$ and $1''.5$, providing a spectral resolution of $R \sim 450$. Figure 5 shows an example of a spectrum obtained in spectropolarimetric mode.

The Stokes parameters for linearly polarized radiation can in this case be determined from the following formulas:

$$I(\lambda) = I_0(\lambda) + I_{90}(\lambda)K_Q(\lambda) + I_{45}(\lambda) + I_{135}(\lambda)K_U(\lambda), \quad (3)$$

$$Q(\lambda) = \frac{I_0(\lambda) - I_{90}(\lambda)K_Q(\lambda)}{I_0(\lambda) + I_{90}(\lambda)K_Q(\lambda)}, \quad (4)$$

$$U(\lambda) = \frac{I_{45}(\lambda) - I_{135}(\lambda)K_U(\lambda)}{I_{45}(\lambda) + I_{135}(\lambda)K_U(\lambda)}, \quad (5)$$

where K_Q and K_U are instrumental parameters, which depend on the transmission of the polarization channels, which, in turn, can be determined from observations of stars with zero polarization. Here $I_0(\lambda)$, $I_{90}(\lambda)$, $I_{45}(\lambda)$, and $I_{135}(\lambda)$ are the measured intensities corresponding to different polarization directions. Polarization degree P and angle PA of the polarization plane are computed from formula (2).

Figure 6 shows the wavelength dependences of the polarization parameters of asteroid 1994 UG: flux $F(\lambda)$ in the spectrum of the object in the 420–800 nm

Table 2. Results of position and photometric measurements of asteroid 1994 UG made on March 7, 2016

File	UT, hh mm ss.ss	$T_{\rm exp}$, s	Filter	z, deg	Seeing, arcsec	RA(2000), hh mm ss.ss	Dec(2000), dd mm ss.ss	Error, arcsec	Magnitude
(1)	(2)	(3)	(4)	(5)	(6)	(7)	(8)	(9)	(10)
s13860101	21:58:31.04	120	B	22	2.0	09 37 44.841	+48 43 06.97	0.17	17.21 ± 0.02
s13860102	22:00:42.07	60	V	22	2.0	09 37 44.117	+48 43 10.31	0.18	16.83 ± 0.02
s13860103	22:02:19.65	30	R	22	2.0	09 37 43.581	+48 43 13.75	0.22	16.59 ± 0.02
s13860104	22:04:08.01	120	B	22	2.0	09 37 42.929	+48 43 17.71	0.25	17.21 ± 0.02
s13860105	22:06:33.26	60	V	23	2.0	09 37 42.066	+48 43 21.68	0.26	16.84 ± 0.02
s13860106	22:07:44.00	30	R	23	2.0	09 37 41.687	+48 43 24.16	0.14	16.59 ± 0.02
s13860107	22:10:59.79	120	B	23	2.0	09 37 40.880	+48 43 28.42	0.27	17.20 ± 0.02
s13860108	22:12:30.51	60	V	24	2.0	09 37 39.996	+48 43 33.77	0.19	16.83 ± 0.02
s13860109	22:13:34.01	30	R	24	2.0	09 37 39.644	+48 43 35.80	0.14	16.58 ± 0.02
s13860110	22:15:22.21	120	B	24	2.0	09 37 38.964	+48 43 39.70	0.25	17.18 ± 0.02
s13860111	22:18:10.04	60	V	25	2.0	09 37 38.058	+48 43 44.66	0.14	16.82 ± 0.02
s13860112	22:20:53.01	30	R	25	2.0	09 37 37.076	+48 43 50.01	0.12	16.62 ± 0.02
s13860113	22:21:04.96	120	B	26	2.0	09 37 36.322	+48 43 54.41	0.20	17.19 ± 0.02
s13860114	22:26:07.70	60	V	26	2.0	09 37 35.270	+48 44 00.58	0.15	16.83 ± 0.02
s13860115	22:28:39.51	30	R	27	2.0	09 37 34.384	+48 44 05.37	0.13	16.61 ± 0.02
s13860116	22:31:14.09	120	B	27	2.0	09 37 33.519	+48 44 10.82	0.23	17.21 ± 0.02
s13860117	22:32:57.34	60	V	27	2.0	09 37 32.905	+48 44 13.98	0.21	16.84 ± 0.02
s13860118	22:34:59.67	30	R	28	2.0	09 37 32.176	+48 44 17.92	0.10	16.58 ± 0.02
s13860119	22:36:57.95	120	B	28	2.0	09 37 31.441	+48 44 22.23	0.26	17.19 ± 0.02
s13860120	22:39:11.78	60	V	28	2.0	09 37 30.661	+48 44 26.27	0.17	16.82 ± 0.02
s13860121	22:40:37.14	30	R	29	2.0	09 37 30.234	+48 44 28.86	0.19	16.62 ± 0.02
s13860122	22:43:43.62	120	B	29	2.0	09 37 29.177	+48 44 35.07	0.19	17.22 ± 0.02
s13860123	22:46:02.01	60	V	30	2.0	09 37 28.358	+48 44 39.43	0.18	16.83 ± 0.02
s13860124	22:47.13.87	30	R	30	2.0	09 37 27.929	+48 44 41.81	0.11	16.61 ± 0.02
s13860125	22:49:54.56	120	B	30	2.0	09 37 26.964	+48 44 47.28	0.20	17.23 ± 0.02
s13860126	22:52:03.73	60	V	30	2.0	09 37 26.209	+48 44 50.86	0.17	16.87 ± 0.02
s13860127	22:53:15.62	30	R	31	2.0	09 37 25.857	+48 44 53.11	0.14	16.60 ± 0.02
s13860128	22:54:51.87	120	B	31	2.0	09 37 25.330	+48 44 56.44	0.11	17.22 ± 0.02
s13860129	22:56:46.85	60	V	31	2.5	09 37 24.647	+48 45 00.29	0.23	16.84 ± 0.02
s13860130	22:58:59.68	30	R	32	2.5	09 37 23.877	+48 45 04.88	0.14	16.62 ± 0.02

corrected for spectral response; normalized Stokes parameters $Q(\lambda)$ and $U(\lambda)$; polarization degree $P(\lambda)$, and the position angle $PA(\lambda)$ of the polarization plane. The solar spectrum in arbitrary units in accordance with international standard ISO 9845-1:1992[1] is shown next to the spectrum of the object. In the spectrum of the asteroid Fraunhofer absorption lines show up conspicuously and the continuum shows appreciable reddening compared to the solar continuum. The broad absorption features at 690 and 760 nm are molecular absorption bands in the Earth's atmosphere. The energy distribution in the spectrum of the asteroid indicates that we are dealing with an S-type asteroid [14]. As is evident from the figure, polarization degree decreases with increasing wavelength. Integration of polarized spectrum in the bands of Johnson's photometric system yields the

[1]http://www.pveducation.org/pvcdrom/appendices/standard-solar-spectra

following polarization degree estimates for different passbands: $P_B = (6.2 \pm 0.6)\%$, $P_V = (3.5 \pm 0.5)\%$, and $P_R = (2.5 \pm 0.3)\%$. Note that the angle of the polarization plane in the wavelength interval considered remains constant to within the measurement errors, as expected for asteroid observations. The phase angle of the asteroid at the time of observations was equal to $46\overset{\circ}{.}5$. Such values of the parameters of asteroid 1994 UG are close to those obtained in broadband polarimetric measurements of the near-Earth asteroid (1685) Toro [7].

The first spectropolarimetric data for bright asteroids were obtained in [15], we are the first to perform spectropolarimetry of faint NEAs. A comparison of the normalized wavelength dependences of polarization with the data obtained for S-type asteroid Eros at the phase angle of 42° (see Fig. 3 in [15]) shows a remarkable similarity with our data. Note that in our case polarization in the V-band is about twice stronger than the corresponding polarization in Eros. This circumstance may indicate that as far as the wavelength variation of albedo and polarization degree are concerned, the properties of the surface of asteroid 1994 UG are close to those of the surfaces of lunar maria [16] at large phase angles.

3. CONCLUSIONS

We performed the first ever spectropolarimetric observations of faint near-Earth asteroids. We showed that 1994 UG is an S-type asteroid and that as far as polarization is concerned, its surface properties are close to those of lunar maria. We found a strong increase of polarization (from 3% to 14%) in the faint asteroid 2009 DL46, which is indicative of the nonuniformity of the surface.

ACKNOWLEDGMENTS

We are grateful to N. N. KIselev for critical comments, and to the administration of the Special Astrophysical Observatory of the Russian Academy of Sciences for allocating time for observations of asteroids. This work was supported by the Russian Foundation for Basic Research (project no. 16-12-00071).

REFERENCES

1. D. Morate, J. de León, M. De Prá, et al., Astron. and Astrophys. **586**, A129 (2016).
2. C. R. Chapman, D. Morrison, and B. Zellner, Icarus **25**, 104 (1975).
3. M. I. Mishchenko, V. K. Rosenbush, N. N. Kiselev, et al., arXiv:1010.1171 (2010).
4. R. P. Binzel, D. Lupishko, M. di Martino, et al., *Physical Properties of Near-Earth Objects* (Univ. Arizona Press, Tucson, 2002), pp. 255–271.
5. S. J. Bus, F. Vilas, and M. A. Barucci, *Visible-Wavelength Spectroscopy of Asteroids* (Univ. Arizona Press, Tucson, 2002), pp. 169–182.
6. D. F. Lupishko and S. V. Vasilyev, NASA Planetary Data System **184**, EAR-A-3-RDR-APD-POLARIMETRY-V7.0 (2012).
7. N. N. Kiselev, D. F. Lupishko, G. P. Chernova, and I. G. Shkuratov, Kinematics and Physics of Celestial Bodies **6**, 77 (1990).
8. M. Ishiguro, H. Nakayama, M. Kogachi, et al., Publ. Astron. Soc. Japan **49**, L31 (1997).
9. I. N. Belskaya, S. Fornasier, and Y. N. Krugly, Icarus **201**, 167 (2009).
10. N. N. Kiselev, V. K. Rosenbush, K. Jockers, et al., in *Proc. Intern. Conf. on Asteroids, Comets, and Meteors — ACM 2002, Berlin, Germany, 2002*, Ed. by B. Warmbein, ESA SP **500** (ESA Publ. Division, Noordwijk, 2002), pp. 887–890 .
11. V. L. Afanasiev and A. V. Moiseev, Baltic Astronomy **20**, 363 (2011).
12. J. L. Russell, B. M. Lasker, B. J. McLean, et al., Astron. J. **99**, 2059 (1990).
13. V. L. Afanasiev and V. R. Amirkhanyan, Astrophysical Bulletin **67**, 438 (2012).
14. E. S. Howell, E. Merenyi, and L. A. Lebofsky, J. Geophys. Research **99**, 10 (1994).
15. S. Bagnulo, A. Cellino, and M. F. Sterzik, Monthly Notices Royal Astron. Soc. **446**, L11 (2015).
16. N. V. Opanasenko and Y. G. Shkuratov, Astronomicheskii Vestnik **28**, 133 (1994).

Translated by A. Dambis